

# DEVELOPMENT OF FLOATING WAVE BARRIERS FOR COST-EFFECTIVE PROTECTION OF IRRIGATION POND LEVEES

Y. Ozeren, D. G. Wren, C. V. Alonso

**ABSTRACT.** *The earth levees commonly used for irrigation reservoirs are subjected to significant embankment erosion due to wind-generated waves. Large seasonal fluctuations in water level make vegetative bank protection impractical, and other stabilization methods, such as the use of stone or discarded tires, are not acceptable due to ecological or economic concerns. Here, a floating wave barrier made of polyethylene irrigation tubing is designed through a laboratory model study and subjected to a short-term prototype-scale field test. Based on wave characteristics measured in an irrigation pond near Carlisle, Arkansas, a laboratory-scale wave generating flume was designed, constructed, and used to test multiple wave barrier configurations for regular waves in deep and transitional water depths. Wave transmission characteristics were investigated for the following breakwater arrangements: (1) fully restrained, (2) vertically restrained with a single mooring line, and (3) horizontally restrained with piles at both sides of the wave barrier. The test results show that cylindrical pipes can be used effectively and that wave transmission characteristics strongly depend on the draft and mooring configuration of the wave barrier. The use of multiple small cylinders to replace a single large one is validated. A composite design made of two sizes of cylinders joined at the top was chosen for field testing. In the prototype-scale field test, wave amplitudes were reduced by an average of approximately 50%, which translates into a 75% reduction in wave energy.*

**Keywords.** *Erosion protection, Levee erosion, Levee protection, Wave erosion.*

Over 50% of the 700 miles of levees that are currently being used for commercial aquaculture and irrigation storage experience significant embankment erosion due to wind-driven waves (Carman, 2003). In irrigation reservoirs, water is stored in the winter and pumped onto crops in the summer, resulting in water levels that fluctuate over several feet, making vegetative bank protection impractical. Bank protection by tires, construction debris, and riprap has been successfully used, but these are not acceptable methods because of ecological and economic concerns (Carman, 2003). Figure 1 shows a typical example of levee erosion in an irrigation pond.

Floating wave barriers are commonly used to protect small marinas and for shoreline erosion control in coastal areas (McCartney, 1985). The kinetic energy of deep water waves, where the wavelength is less than half the water depth, is concentrated near the water surface, making it possible to use floating structures to reduce wave energy. Wave attenuation is primarily achieved by reflection and dissipation of the incoming wave energy. Floating wave barriers have lower construction costs and shorter construction times than bottom mounted structures and are suitable for locations where wave conditions are not severe and the water depth is high relative to the length of waves. The relatively short fetch length

(approx. 400 to 800 m) and wave periods (1 to 2 s) in most irrigation ponds are suitable conditions for using floating wave barriers (Werner, 1988). Floating wave barriers can also accommodate the depth changes that are required for the operation of irrigation reservoirs.

A large variety of floating wave barrier configurations has been developed for coastal applications. These structures can be classified according to their geometric configuration and functionality (Hales, 1981; McCartney, 1985). Either piles or mooring lines are typically used to restrain the breakwater motions. The choice of wave barrier type depends primarily on local wave characteristics, foundation conditions, and the availability of construction materials. Floating wave barriers have proven to be effective wave-attenuation devices, but they must be designed carefully to serve well in specific applications (Isaacson, 1993).

The general design of floating breakwaters for use in marine environments is well developed. For reviews of past work relevant to floating wave barriers, the reader is directed to the following publications: Hales (1981), Richey and Nece (1974), McLaren (1981), McCartney (1985), Werner (1988), and Isaacson (1993). In spite of the large amount of work on coastal applications, a specific design for low-cost levee protection in small reservoirs was lacking. The goal of the current work is to provide an inexpensive wave barrier design that can be implemented by landowners using commonly available materials. For this reason, a design that utilizes cylindrical pipe sections was sought, with plans to use inexpensive polyethylene irrigation tubing for the final field implementation.

Levee erosion by waves is controlled by wave properties and bank materials. Because of the wide range of soil types in levee embankments, the current study focused on reducing wave energy, which, for any soil type or levee configuration,

---

Submitted for review in January 2008 as manuscript number SW 7338; approved for publication by the Soil & Water of ASABE in August 2008.

The authors are **Yavuz Ozeren**, Graduate Student, Department of Civil Engineering, University of Mississippi, Oxford, Mississippi; **Daniel G. Wren**, Hydraulic Engineer, and **Carlos V. Alonso**, Hydraulic Engineer, USDA-ARS National Sedimentation Laboratory, Oxford, Mississippi. **Corresponding author:** Daniel G. Wren, P.O. Box 1157, Oxford, MS 38655; phone: 662-232-2329; fax: 662-281-5706; e-mail: Daniel.Wren@ars.usda.gov.



Figure 1. South shore of the irrigation reservoir illustrates extensive erosion damage.

should decrease erosion. Lower amplitude, less energetic waves have been shown to cause less erosion than higher amplitude waves (CERC, 2003). The results from this study show that wave barrier effectiveness improves as wave height relative to barrier diameter decreases. Therefore, protecting the shoreline from high-amplitude waves will also protect it from low-amplitude waves. Even though low-amplitude waves often occur over longer time periods than larger waves, there will be little or no levee damage until some critical shear stress is exceeded. This is one reason why some levees may stand with little damage for years but then sustain substantial damage from one strong storm (USDA-SCS, 1974).

The description of the work is divided into three sections. First, preliminary field data collection on wind and wave characteristics is described. Second, the model-scale laboratory work used to study the interactions between waves and breakwaters is described. Third, a brief description of the results from a short-term prototype-scale field study is presented. The main objective of the present work is to demonstrate that floating wave barriers are a viable option for low-cost protection of earth levees. A successful design is presented, but further research will be required before it is possible to present full guidelines for large-scale field implementation.

## MATERIALS AND METHODS

### FIRST FIELD STUDY

In March 2005, a temporary wind and wave monitoring station was deployed in an irrigation reservoir approximately 10 km east of Carlisle, Arkansas, so that wind-driven wave characteristics could be measured for use in scaling the model study. The reservoir dimensions were  $770 \times 370$  m. The prevalent wind direction was observed to be from the north-

east, so the measurement tower was positioned in the southwest corner of the reservoir in order to maximize the fetch length. The water depth,  $h$ , at the installation point was 2.5 m. Bathymetric variations were negligible in the vicinity of the measuring station. Approximately 110 min of concurrent wind direction, wind speed, and wave height data were collected. The wind conditions were high, averaging approximately  $48 \text{ km h}^{-1}$  during the data collection period. Thus, it was appropriate to use the measured wind and wave conditions as a basis for designing the model-scale experiments.

Water level measurements were made using two ultrasonic distance sensors separated by a fixed distance, aligned roughly parallel to the observed wind direction and mounted approximately 35 cm above the mean water level. The ultrasonic distance sensors collected data at a rate of 10 Hz. The time series of surface elevations was analyzed by both time domain (wave train) and frequency domain (spectral) analysis. The water surface elevation signal was divided into segments of 4096 data points, which corresponds to 6.83 min for 10 Hz data recording. Each data segment was analyzed with 50% of the data overlapping the previous segment. Spectral analysis was performed on 512-point subsegments (51.2 s), again with 50% overlapping. Then, eight wave spectra within each segment were averaged for each frequency band to get the average spectrum along the 6.83 min interval. Figure 2 is the average spectrum for 60 min of data, including a comparison with the JONSWAP wave spectrum (CERC, 2003). The good agreement with the JONSWAP spectrum serves to validate the data collection and analysis methods used here.

Time domain analysis of data sets with 4096 points (6.83 min) using the zero downcrossing method was also performed (CERC, 2003). The zero crossing significant wave height,  $H_s$ , is the average of the highest one-third of the waves in a record.  $H_s$  was 4.5% lower than the spectral estimate for

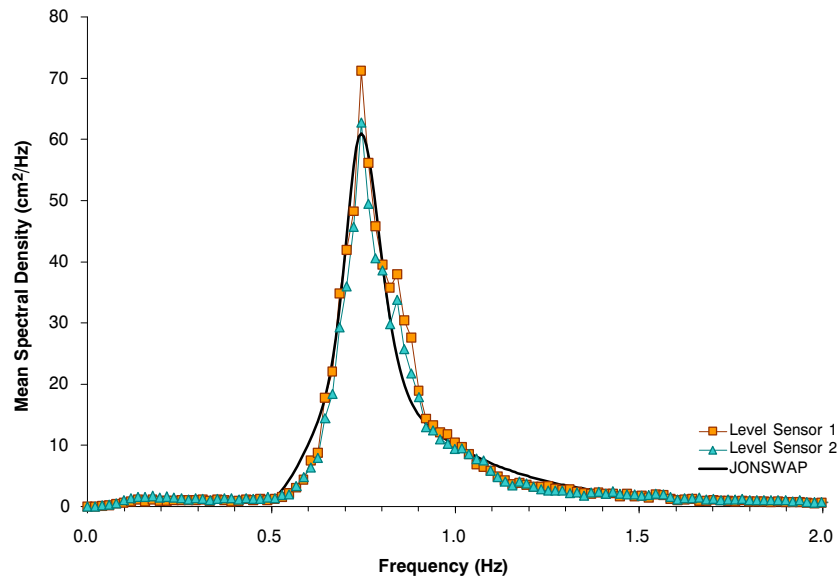


Figure 2. Average spectrum for 60 min data recording with an interval length of 512 data points.

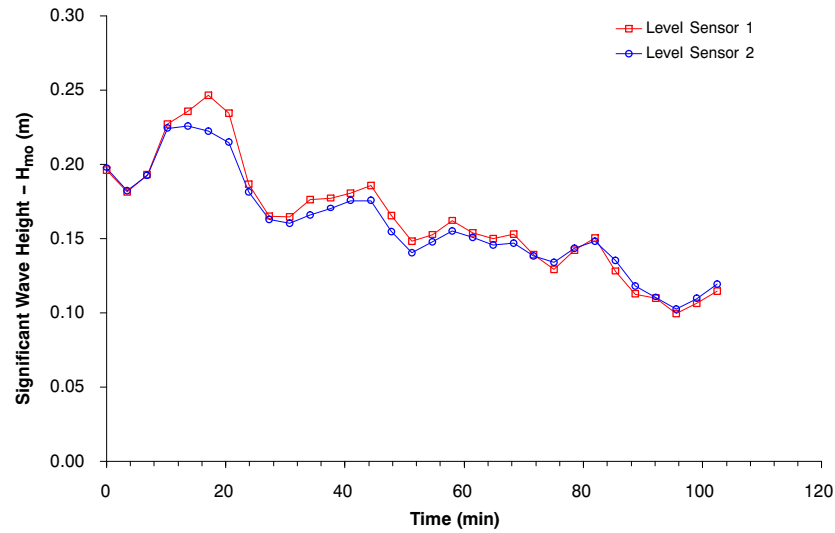


Figure 3. Significant wave height estimated from the wave spectrum for the entire data set.

Table 1. Ranges of experimental parameters.

| Restraint | Model | Vertical Length, $d$ (mm) | Horizontal Length, $b$ (mm) | Draft, $z_d$ (mm) | Water Depth, $h$ (mm) | Wave Height, $H$ (mm) | Wave Period, $T$ (s) | Incident Wave Steepness, $H_i/L$ | Relative Depth, $kh$ | Aspect Ratio, $z_d/d$ |
|-----------|-------|---------------------------|-----------------------------|-------------------|-----------------------|-----------------------|----------------------|----------------------------------|----------------------|-----------------------|
| Fixed     | 61    | 114.6                     | 114.6                       | 24.3              | 446                   | 15 - 45               | 0.5 - 1.3            | 0.006 - 0.08                     | 1.3 - 7.5            | 0.5                   |
|           | 62    | 114.6                     | 114.6                       | 57.3              | 466                   | 16 - 75               | 0.6 - 1.2            | 0.03 - 0.08                      | 1.4 - 5.2            | 1.0                   |
|           | 63    | 114.6                     | 114.6                       | 80.2              | 446                   | 17 - 75               | 0.6 - 1.3            | 0.03 - 0.08                      | 1.4 - 7.5            | 0.7                   |
|           | 91    | 112.3                     | 120.4                       | 82.2              | 446                   | 20 - 45               | 0.5 - 1.2            | 0.009 - 0.1                      | 1.3 - 7.5            | 0.7                   |
| Moored    | 64    | 114.6                     | 114.6                       | 57.3              | 446                   | 15 - 50               | 0.5 - 1.2            | 0.006 - 0.08                     | 1.4 - 7.5            | 0.5                   |
|           | 65    | 114.6                     | 114.6                       | 57.3              | 446                   | 15 - 50               | 0.5 - 1.3            | 0.006 - 0.08                     | 1.3 - 7.5            | 1.0                   |
| Piles     | 59    | 89                        | 89                          | 83.4              | 466                   | 12 - 78               | 0.5 - 1.3            | 0.02 - 0.08                      | 1.3 - 7.5            | 1.0                   |
|           | 60    | 114.6                     | 112                         | 57.3              | 446                   | 10 - 78               | 0.5 - 1.2            | 0.02 - 0.08                      | 1.4 - 7.5            | 0.5                   |
|           | 69    | 114.6                     | 114.6                       | 110.0             | 446                   | 12 - 78               | 0.5 - 1.3            | 0.01 - 0.08                      | 1.3 - 7.5            | 1.0                   |
|           | 70    | 114.6                     | 114.6                       | 81.6              | 446                   | 10 - 78               | 0.5 - 1.3            | 0.02 - 0.08                      | 1.4 - 7.5            | 0.7                   |
|           | 96    | 114.6                     | 300                         | 89                | 466                   | 12 - 78               | 0.5 - 1.3            | 0.02 - 0.08                      | 1.3 - 7.5            | 1.0                   |

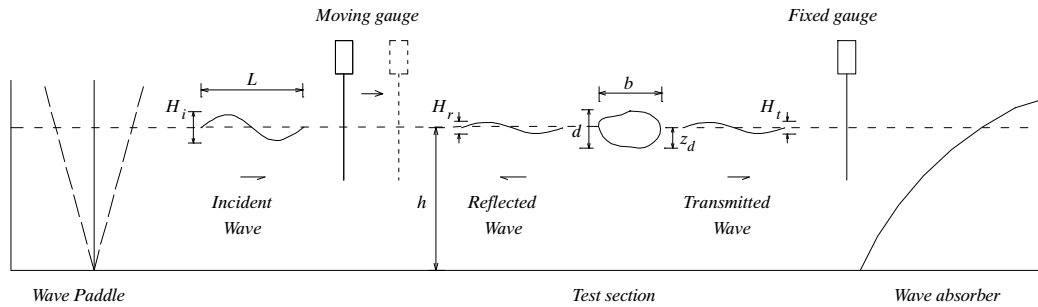


Figure 4. Diagram of wave flume and definition of key variables.

the significant wave height,  $H_{mo}$ , shown in figure 3, a difference that is reasonable based on similar measurements by others (Longuet-Higgins, 1980).

#### MODEL STUDY

Wave barrier models were scaled by selecting the size of the model and then adjusting the wave parameters so that the Froude scaling criterion was satisfied (Hughes, 1993). This resulted in a ratio of prototype to model length scale of approximately 1:3. Table 1 shows ranges of parameters used in the model study, and variables are defined graphically in figure 4. The Reynolds number was approximately  $10^5$  to  $10^6$ , which is high enough to render the difference between model and prototype scales negligible; therefore, the Reynolds scaling criterion was not used (Hughes, 1993). The wave gauges were positioned far enough from the breakwater to avoid local disturbances due to viscous effects in both the field and experimental studies.

In climate data compiled by the USDA-NRCS National Water and Climate Center for the Little Rock, Arkansas National Airport approximately 40 miles west of the study site,

it was found that winds over  $40 \text{ km h}^{-1}$  occurred less than 2% of the time January to April and less than 1% of the time for the rest of the year. The wave characteristics used to scale the model study were determined from field data that were collected in the presence of sustained winds up to  $48 \text{ km h}^{-1}$ , which exceeds typical wind conditions except in a few of the most extreme events.

A 19 m wave flume with a computer-controlled flap-type wave generator and wire mesh permeable wave absorber was designed and constructed at the USDA-ARS National Sedimentation Laboratory. Figure 5 shows the flume, wave generator, and wave absorber. The relationship between the motion of the wave generator and the generated wave properties was obtained experimentally and found to be in good agreement with first-order wave maker theory for the range of wave parameters in the current work (Dean and Dalrymple, 1991). A permeable sloping beach with a parabolic cross-section was used to dissipate wave energy at the end of the flume opposite the wave generator. Reflection from the wave absorber was less than 10% for waves within the experimental range.

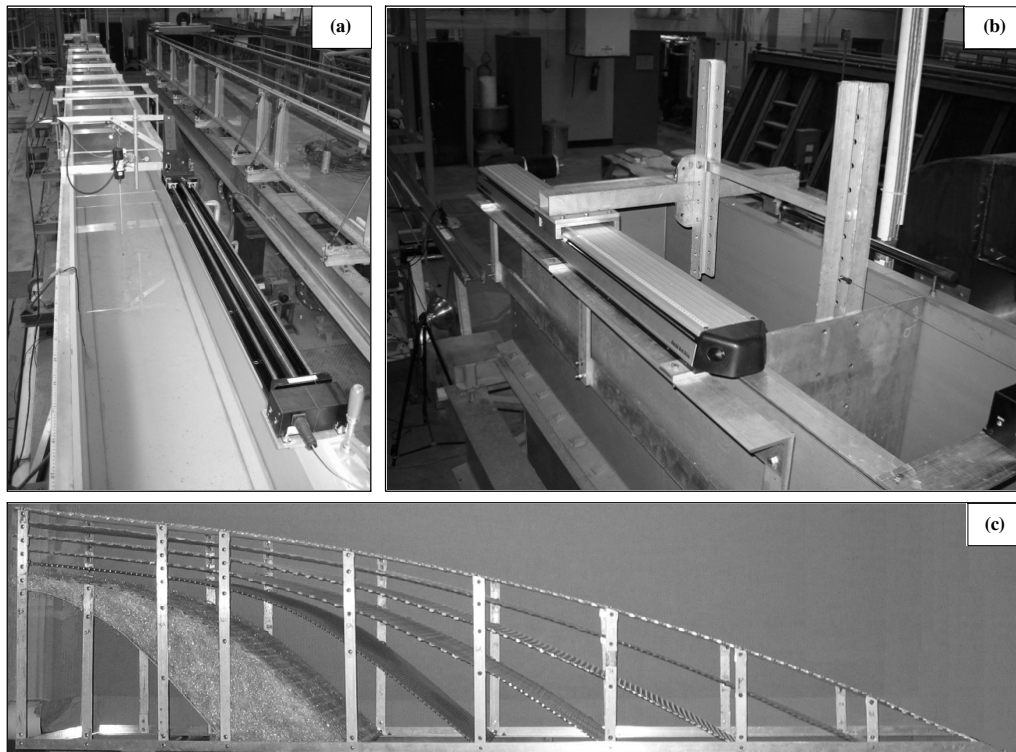


Figure 5. (a) Wave flume, (b) flap type wave generator, and (c) wave absorber.

The interaction of waves with a floating breakwater of an arbitrary shape will result in a portion of the wave energy being reflected from the absorber, a portion of the energy being transmitted through and under the breakwater, and a portion of the wave energy being dissipated by the motion of the wave barrier and turbulence. Incomplete reflections from an obstacle will form a partial standing wave, and the resulting envelope of the wave amplitudes will have stationary points of maximum ( $H_{\max}$ ) and minimum ( $H_{\min}$ ) wave amplitude. The reflection produces a stationary spatial envelope of wave heights given by:

$$H_{\max} = H_i + H_r \quad (1)$$

$$H_{\min} = H_i - H_r \quad (2)$$

where  $H_i$  is the incoming wave height, and  $H_r$  is the reflected wave height. The reflection coefficient,  $\kappa_r$ , can be rewritten in terms of this spatial envelope:

$$K_r = \frac{H_{\max} - H_{\min}}{H_{\max} + H_{\min}} \quad (3)$$

A capacitive level sensor was translated in the direction of wave motion at a velocity sufficient to record at least two envelopes over a 147 cm section of the wave flume to capture the quasi-antinodes and quasi-nodes. A second static level sensor located on the side of the wave barrier opposite the wave generator was used to measure the transmitted wave characteristics. The capacitance level sensors measured the water level at a rate of 30 Hz with an accuracy of approximately  $\pm 1$  mm.

PVC pipes of different circular cross-section, oriented parallel to wave crests, were used as model wave barriers. Fixed, moored, and pile-restrained barriers were tested. In the fixed configuration, the barrier was completely fixed, with no motion allowed. This case is not feasible for field use and was included only for comparison with floating cases and to theory for validation purposes. It was also used for validating data collection and analysis methods by comparing it to previous work by Dean and Ursell (1959). For the sake of brevity, the comparison is not shown here. Models were installed 12.4 m from the wave generator, allowing enough space to take measurements on both sides of the model. The initial position for the moving gauge was 9.6 m and the final position was at most 11 m from the wave generator. The fixed

gauge was installed 13.8 m from the paddle. Both of the level sensors were positioned so that the midpoint of the staff was at mean water level. A computer-controlled system was used to automatically conduct multiple experiments while varying the wave parameters over a specified range. A constant water depth of 466 mm was used for all experiments.

In the moored configuration, the barrier was connected to the bottom of the flume with a single cable. The pipes were slightly shorter (5 mm on each end) than the channel width to avoid side friction, and the ends were sealed to exclude water and facilitate positioning in the wave channel. The draft was adjusted by changing the tension of the mooring line. Excess buoyancy provided tension in the mooring line. An important disadvantage of the moored system is that it cannot accommodate water depth changes. At lower depths, the mooring line becomes loose, and at higher depths, the wave barrier may become fully submerged, resulting in a high transmission coefficient.

Pile-restrained models utilized a pair of vertical rods on each end of the barrier to maintain the model's position. The density of the pipes was adjusted using styrofoam caps at both ends. The remaining volume was filled with water to increase the inertia. The circular pipe sections were completely restrained in the horizontal direction, but they were free to move vertically and roll. Piles have advantages over moored breakwaters since they can easily accommodate water level changes and sustain the desired draft. The restraint provided by the piles is significantly greater than that provided by mooring lines. Two different pile-restrained model configurations are shown in figure 6.

Composite breakwater models, constructed by connecting two or more pipe sections with different geometries, were also tested for each class of restraint. The first pipe was fully submerged, while the second one was 50% submerged. Only the first pipe was restrained between the piles. The rigid connection between the two pipes prevented horizontal movement of the second pipe and rolling motion of both pipes. The gap between the two pipes provided a confined region for overtopped waves to dissipate. The data for each set of experiments were analyzed using computer code developed in-house. A band pass Butterworth filter was used to remove unwanted frequency components. Transmitted and envelope wave periods were obtained by using frequency domain analysis. The wave period for the envelope was corrected with the speed of the moving gauge. The amplitudes were calculated

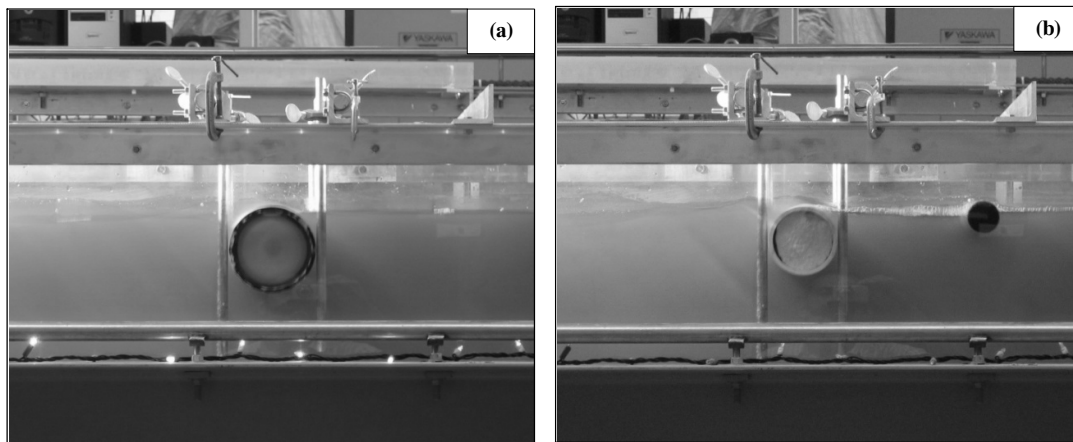


Figure 6. General configurations of pile-restrained wave barriers for (a) a fully submerged single pipe and (b) two pipes connected with rigid bars.

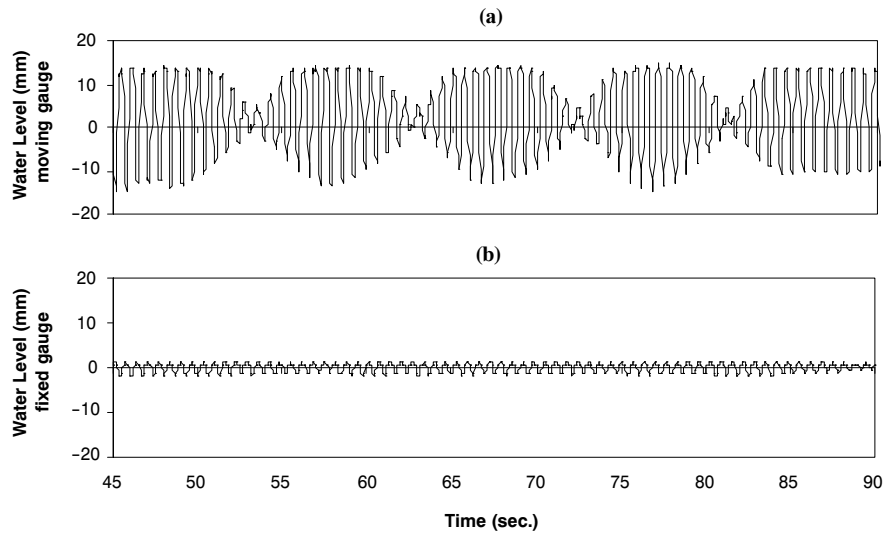


Figure 7. Sample data for  $h = 446.5$  mm,  $H = 20$  mm,  $T = 0.65$  s, and  $d = 114.6$  mm: (a) water level from the moving gauge, and (b) water level from the fixed gauge.

by locating the peaks of the time series data. The maximum and minimum amplitudes of the wave envelope were computed similarly. A sample of data recorded during an experiment is given in figure 7.

## RESULTS AND DISCUSSION

The main objective of the work was to create an effective and economical floating wave barrier. A model study was used to evaluate the effect of different combinations of the controlling variables and to identify a simple design that retained adequate wave damping qualities. Since wave barriers are used to reduce wave height, the primary dependent variable is the transmitted wave height. The energy balance equation for the physical process of a wave encountering a floating breakwater can be stated in terms of wave heights as:

$$\left(\frac{H_r}{H_i}\right)^2 + \left(\frac{H_t}{H_i}\right)^2 + \left(\frac{H_l}{H_i}\right)^2 = 1 \quad (4)$$

where  $H_l$  is the wave height related to energy loss (a derived height representing a quantity of energy lost), and  $H_t$  is the transmitted wave height. Equation 4 can be restated in terms of coefficients:

$$\kappa_r^2 + \kappa_t^2 + \kappa_l^2 = 1 \quad (5)$$

where

$$\kappa_r = \left(\frac{H_r}{H_i}\right) = \text{reflection coefficient} \quad (6)$$

$$\kappa_t = \left(\frac{H_t}{H_i}\right) = \text{transmission coefficient} \quad (7)$$

$$\kappa_l = \left(\frac{H_l}{H_i}\right) = \text{loss coefficient (CERC, 2003)} \quad (8)$$

The most common parameter used to characterize floating breakwater performance is the transmission coefficient,  $\kappa_t$ .

When a floating object with length  $d$  (the diameter in the case of a cylinder) and depth of submergence  $z_d$  interacts with waves of height  $H_i$  and length  $L$  at water depth  $h$ , some portion of the wave energy is transmitted above, below, or through the wave barrier, and some of the energy is reflected or dissipated according to the relationship given in equation 5. The amount of transmitted energy depends on the wave barrier configuration and wave characteristics. Key parameters in the design of a floating wave barrier are the relative submergence ( $z_d/d$ ), the geometry of the barrier, and the method of restraint. The most important wave characteristics are the wave height given as the wave steepness ( $H_i/L$ ) and the wave length given as the relative depth ( $kh$ , where  $k = 2\pi/L$ ). All models in the current study were subjected to a broad range of wave steepnesses.

The data presented in following sections are organized by relative submergence,  $z_d/d$ , geometry, and restraint type.

### EFFECT OF RELATIVE SUBMERGENCE

The effect of relative submergence ( $z_d/d$ ) for fixed, moored, and pile-restrained configurations was tested. Figure 8 presents averaged transmission coefficients (symbols) over a range of wave steepnesses (indicated by bars) for three different submergence ratios of fixed cylindrical pipe sections. Longer waves (small  $kh$ ) were transmitted through the models. The wave barriers were more efficient for shorter waves since the energy concentration was closer to the water surface. As  $z_d/d$  decreased, the amount of reflection increased and transmission decreased. As  $z_d/d$  was increased, waves began to go over the top of the wave barrier. The lack of wave barrier surface area above the water surface limited the ability of the fully submerged cylinder to block waves. In the design range,  $2 < kh < 8$ , the model with  $z_d/d = 0.7$  had the lowest transmission coefficient. This effect is less pronounced for longer waves since the portion of the energy transmission through overtopping is relatively lower.

In figure 9, moored pipes were tested for  $z_d/d = 0.5$  and  $z_d/d = 1.0$ . Here, the fully submerged model performed best, with a decreased transmission coefficient relative to the half-submerged model. The performance of the fully submerged cylinder was found to be more dependent on wave steepness

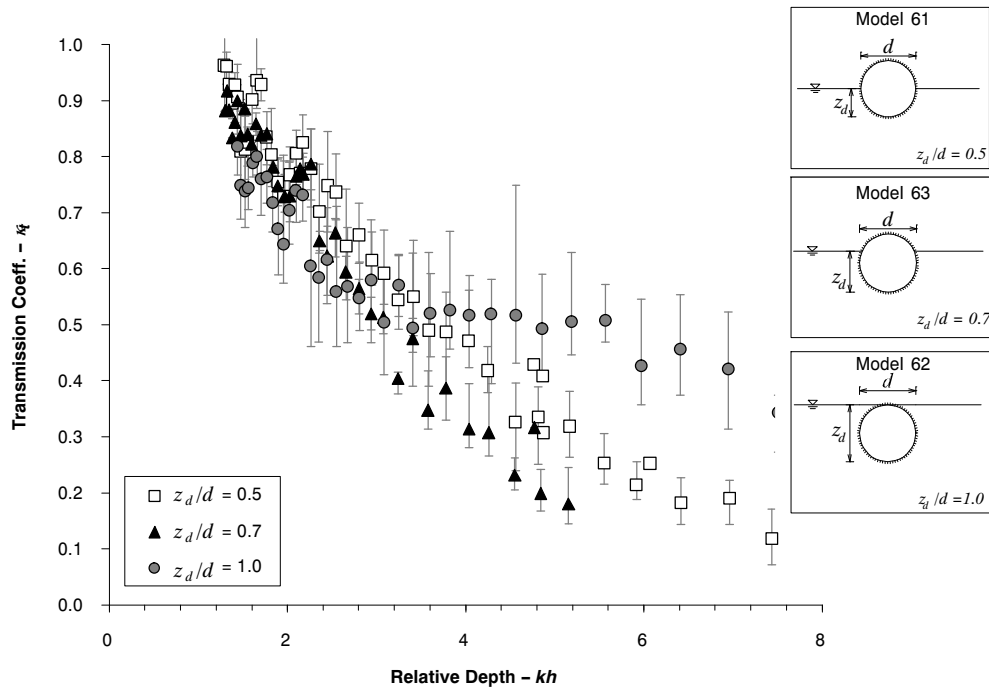


Figure 8. Effect of submergence ratio (aspect ratio) on transmission coefficient for fixed pipe with  $d = 114.6$  mm. Bars represent the range of wave steepness,  $k = 2\pi/L$ , and  $h =$  water depth. See equation 5 for definition of  $\kappa_t$ .

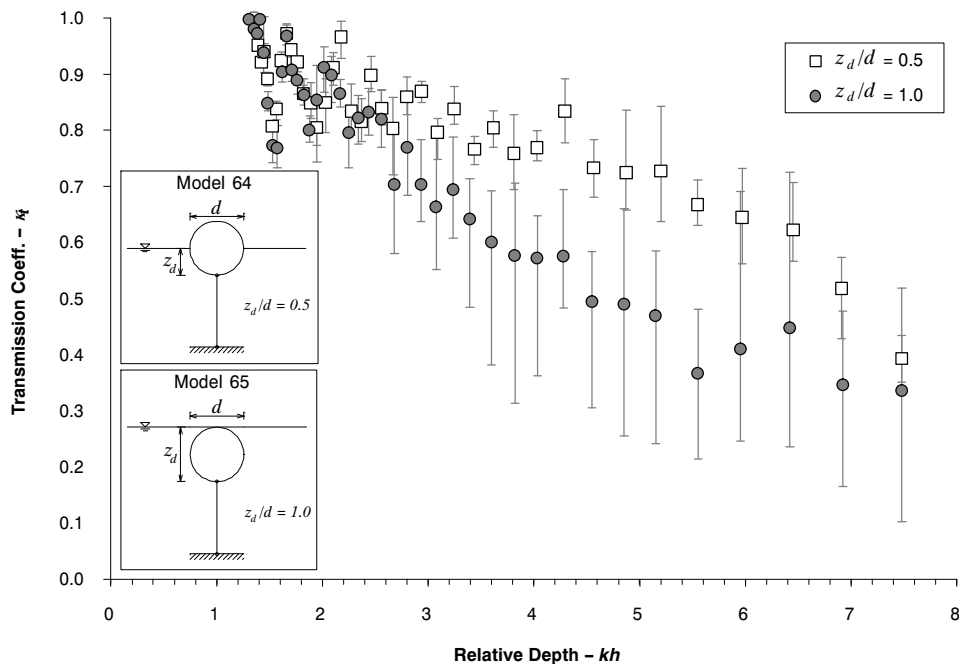


Figure 9. Effect of submergence ratio (aspect ratio) on transmission coefficient for moored pipe with  $d = 114.6$  mm. Bars represent the range of wave steepness,  $k = 2\pi/L$ , and  $h =$  water depth. See equation 5 for definition of  $\kappa_t$ .

due to overtopping, denoted by the wide range of  $\kappa_t$  values caused when the wave steepness was varied. There is a significant increase in  $\kappa_t$  relative to the fixed case due to a method of restraint that allowed a significant amount of motion.

In figure 10, the results of testing pile-restrained wave barrier models with three different  $z_d/d$  values are shown. The highest efficiency is at  $z_d/d = 0.7$ , which provides optimum draft, inertia, and resistance to wave overtopping. This is because wave generation by the vertical motion of the breakwater is decrease due to the increased inertia relative to  $z_d/d =$

0.5. The additional freeboard relative to the fully submerged model decreased overtopping for most of the waves within the experimental range. The pile-restrained model with  $z_d/d = 0.7$  also demonstrated higher reflection coefficients than other tested  $z_d/d$  values.

#### EFFECT OF GEOMETRY

A bundle of smaller pipes can be substituted for a larger cylinder to reduce the material and transportation costs. The advantages of using smaller pipes are discussed more fully

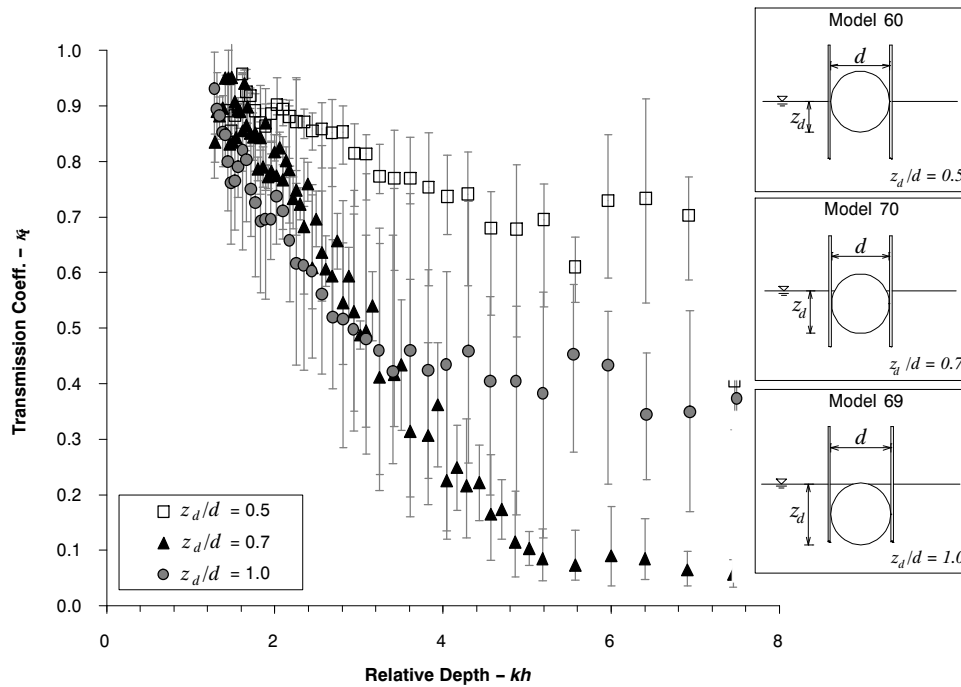


Figure 10. Effect of submergence ratio (aspect ratio) on transmission coefficient for pile-restrained pipe with  $d = 114.6$  mm. Bars represent the range of wave steepness,  $k = 2\pi/L$ , and  $h =$  water depth. See equation 5 for definition of  $\kappa_r$ .

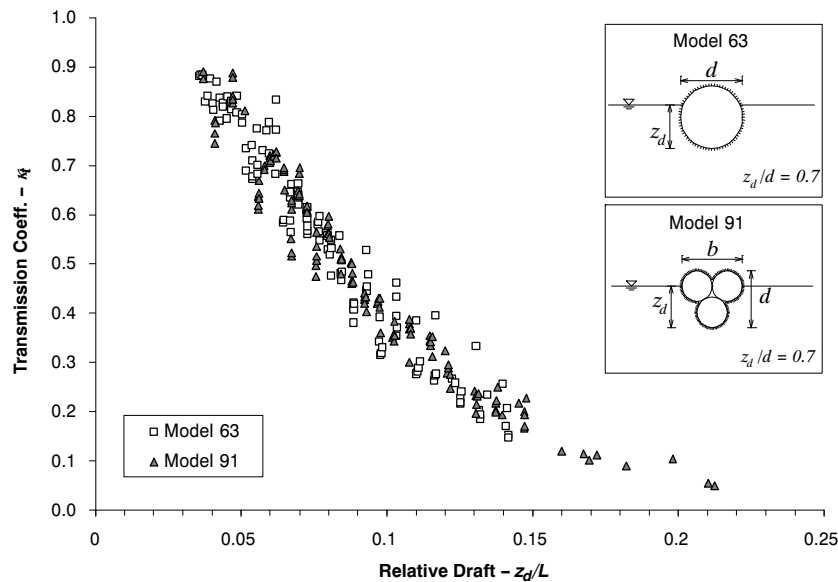


Figure 11. Comparison of transmission coefficients of fixed single pipe and bundle of three pipes;  $z_d =$  submerged portion of wave barrier, and  $L =$  length of incident wave. See equation 5 for definition of  $\kappa_r$ .

below. Here, it is demonstrated that bundles are as effective as larger pipes with similar diameter. In figure 11, the transmission coefficient of the fixed single pipe and a bundle with aspect ratio  $z_d/d = 0.7$  are compared. The transmission coefficients of the two models are similar, indicating that the shape of the cylinder had little influence on the efficiency of the wave absorber for the same relative submergence. The effect of using a corrugated irrigation pipe instead of the smooth PVC pipes used in the model runs was also tested, resulting in the conclusion that the corrugations had no negative impact on wave barrier efficiency. In figure 11 (and in figs. 12 through 15), the  $x$ -axis is scaled by relative draft,

$z_d/L$ , where  $z_d$  is the submerged depth of the floating barrier, and  $L$  is the length of the incident wave. This scaling allows the effect of pipe diameter relative to wave scale to be seen.

In figure 12, the wave transmission of a single pipe is compared to a composite arrangement utilizing two pipe diameters (see diagram on figure) connected at the top for wave steepnesses of 0.03, 0.06, and 0.08. There is improvement in the efficiency of the composite wave barrier at high wave steepness due to energy dissipated by trapped waves breaking in between the two pipes. The smaller pipe helps to limit the transmission of steeper waves that pass the first by overtopping, while the first pipe provides maximum damping and

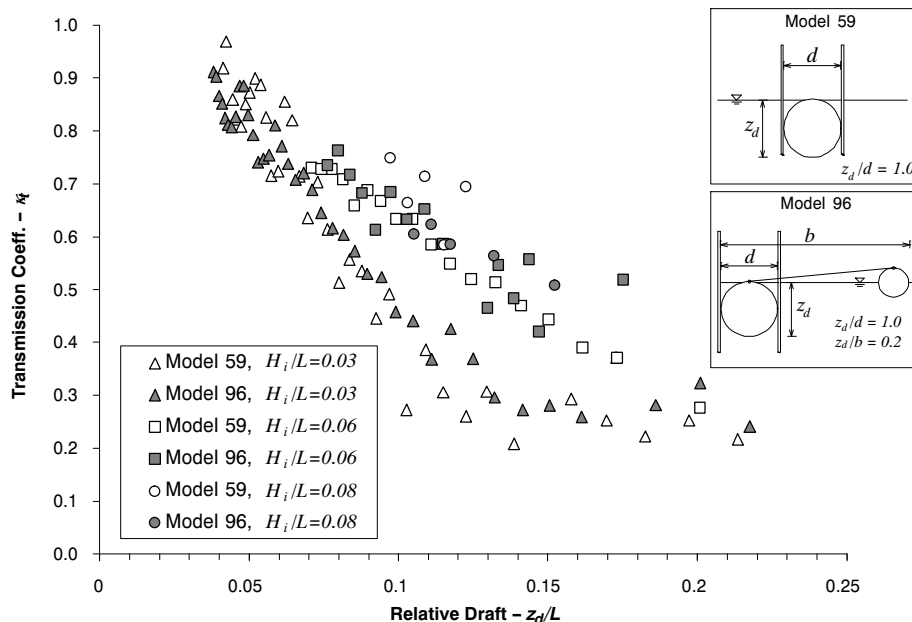


Figure 12. Comparison of transmission coefficients of single and double pipe pile-restrained breakwater models for wave steepness,  $H_i/L = 0.03, 0.06,$  and  $0.07$ ;  $z_d$  = submerged portion of wave barrier; and  $L$  = length of incident wave. See equation 5 for definition of  $\kappa_T$ .

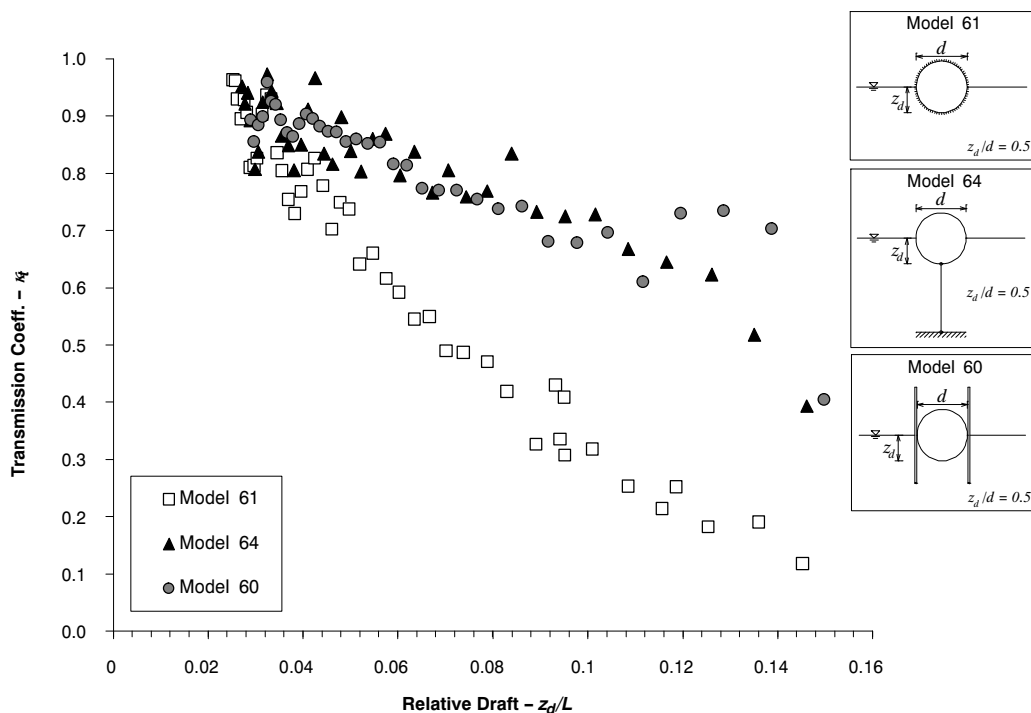


Figure 13. Comparison of the transmission coefficients of half-submerged ( $z_d/d = 0.5$ ) fixed, moored, arm-restrained, and pile-restrained breakwater models with  $d = 114.6$  mm;  $z_d$  = submerged portion of wave barrier, and  $L$  = length of incident wave. See equation 5 for definition of  $\kappa_T$ .

draft that limit the transmission of less steep waves. The advantage of the two-pipe system is seen at higher wave steepness, and this is usually important during the extreme wave conditions that likely cause much of the damage seen on levees. The composite arrangement also provided a ready means for holding the wave barrier in place using the pile located between the two sections.

#### EFFECT OF RESTRAINT TYPE

In figure 13, the wave transmission characteristics of different restraint methods are shown for half-submerged

$z_d/d = 0.5$ ) single-cylinder models with  $d = 114$  mm. Each data point represents the average transmission coefficient over the range of wave steepness. Neither of the partially restrained models are as efficient as the fixed breakwater for  $z_d/d = 0.5$ . In figure 14, the reflection coefficients are compared. It can be seen that the pile-restrained breakwater model has relatively low reflection coefficients, indicating that it reduces wave energy through energy dissipation rather than reflection.

When the pipe section is submerged completely, as in figure 15, the pile-restrained models become more efficient than

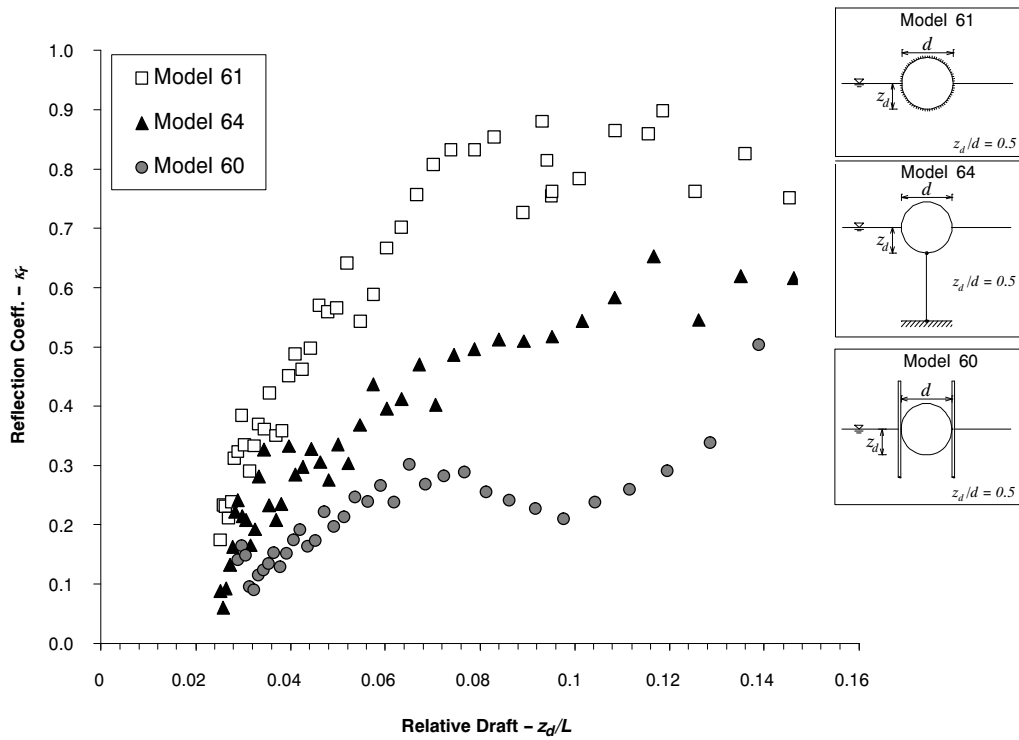


Figure 14. Comparison of the reflection coefficients of half-submerged ( $z_d/d = 0.5$ ) fixed, moored, and pile wave barrier models with  $d = 114.6$  mm;  $z_d$  = submerged portion of wave barrier, and  $L$  = length of incident wave. See equation 5 for definition of  $\kappa_r$ .

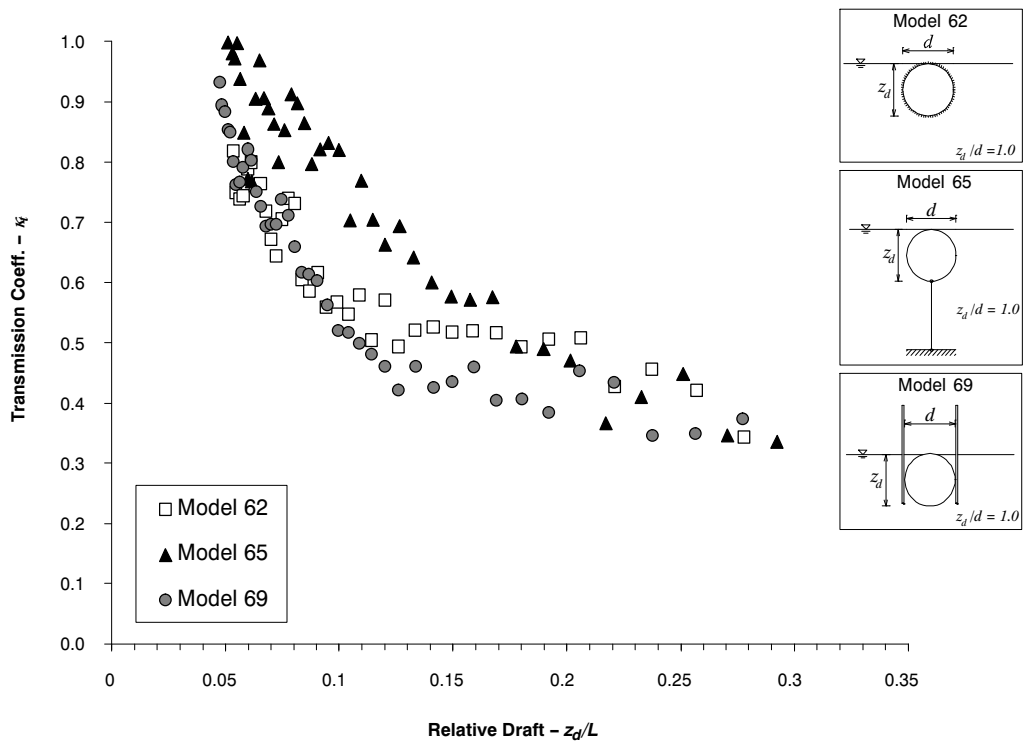


Figure 15. Comparison of the transmission coefficients of fully submerged ( $z_d/d = 1.0$ ) fixed, moored, and pile-restrained breakwater models with  $d = 114.6$  mm;  $z_d$  = submerged portion of wave barrier, and  $L$  = length of incident wave. See equation 5 for definition of  $\kappa_t$ .

the fixed model. For the fully submerged cylinder, energy transmission during overtopping becomes significant, and the dynamic properties of the partially restrained models improve the transmission characteristics of the wave barrier. Note that the data points are averaged over the steepness

range, and for milder waves the transmission coefficients of the pile-restrained model are lower than the average trend, while the transmission coefficients of the fixed model do not change significantly with wave steepness.

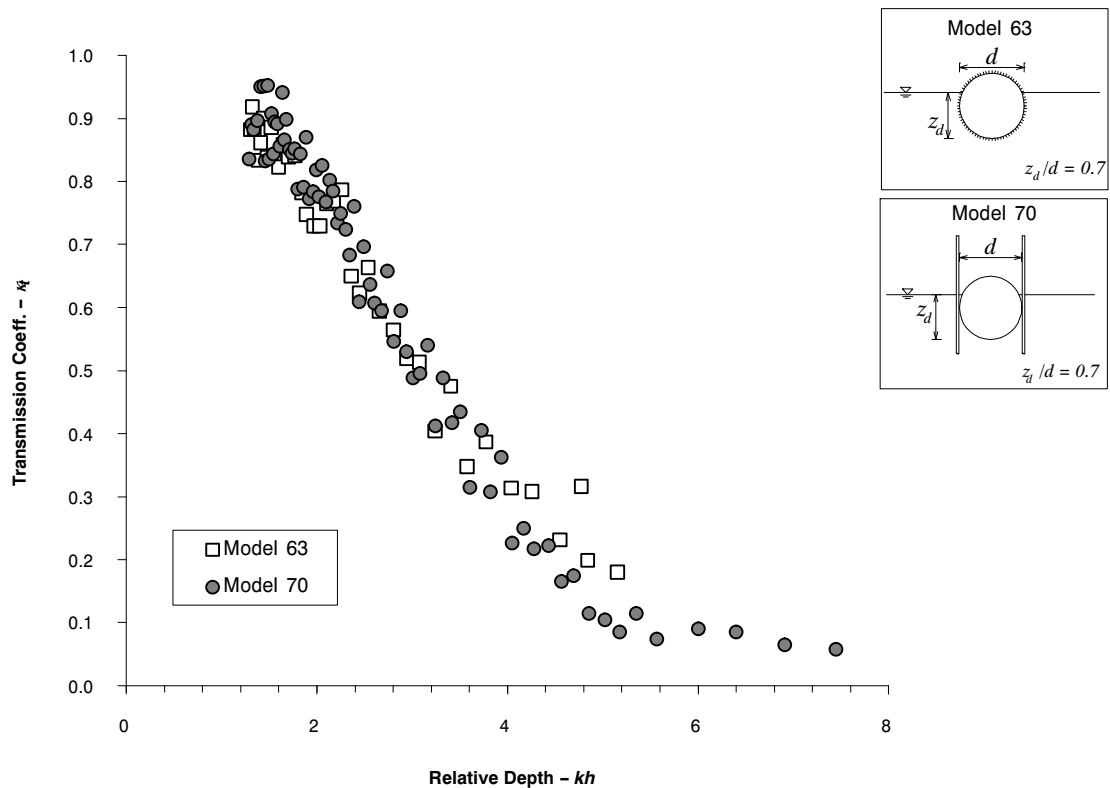


Figure 16. Comparison of the transmission coefficients of partially submerged ( $z_d/d = 0.7$ ) fixed and pile-restrained wave barrier models with  $d = 114.6$  mm;  $k = 2\pi/L$ , and  $h =$  water depth. See equation 5 for definition of  $\kappa_t$ .

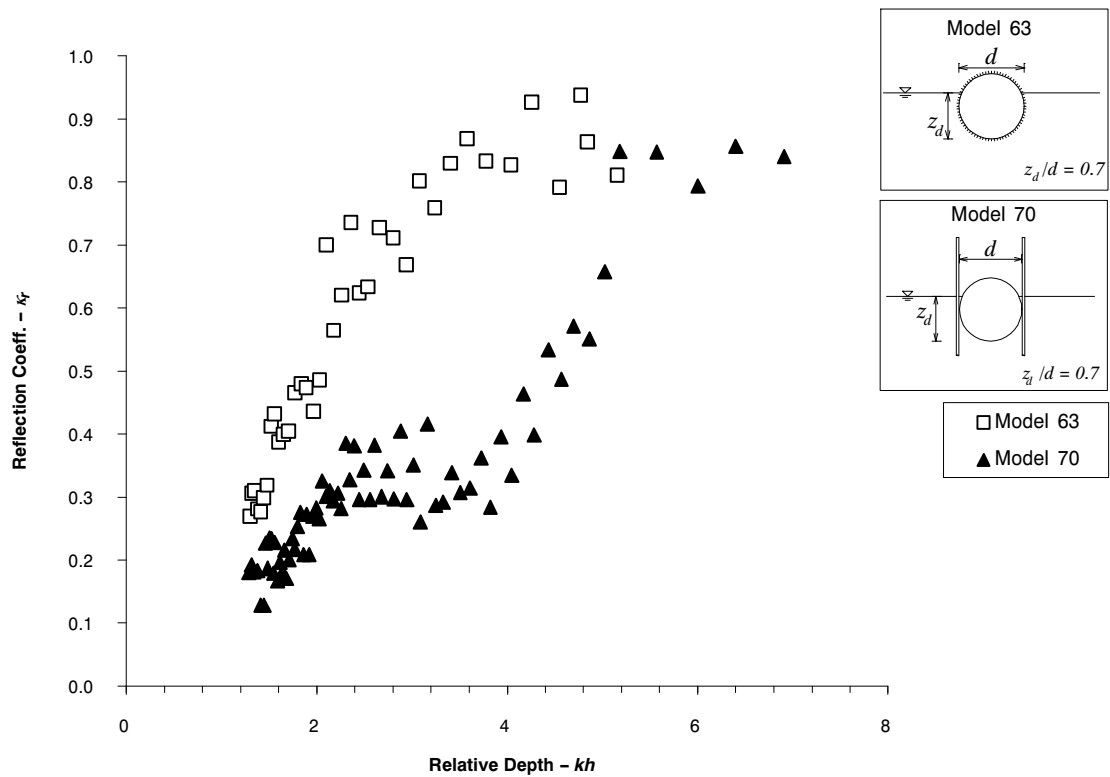


Figure 17. Comparison of the reflection coefficients of partially submerged ( $z_d/d = 0.7$ ) fixed and pile-restrained wave barrier models with  $d = 114.6$  mm;  $k = 2\pi/L$ , and  $h =$  water depth. See equation 5 for definition of  $\kappa_r$ .

In figure 16, the transmission coefficients of fixed and pile-restrained partially submerged ( $z_d/d = 0.7$ ) models are compared. The pile-restrained configuration has transmission coefficients as low as the fully restrained model. In figure 17, it can be seen that the reflection coefficients of the pile-restrained breakwater are lower than the fully constrained configuration even though their transmission characteristics are similar, indicating again that the main mechanism of wave attenuation for the pile-restrained model is energy dissipation. When the waves get shorter ( $2.5 < kh < 4.5$ ), the reflection coefficients of the pile-restrained model do not increase as rapidly as the fixed model, since some of the energy is damped when the waves interact with the partially restrained cylinder. For  $kh > 4.5$ , the dynamic response of the pile-restrained breakwater becomes insignificant, and it responds like the fixed model.

#### FINAL DESIGN AND RESULTS FROM FIELD TEST

Based on the results of the model study, two wave barrier configurations were chosen for prototype-scale field testing in the same reservoir where the preliminary wave characteristics were measured. One utilized a single 29 cm polyethylene irrigation pipe, and the second was a composite design made up of one standard 24 cm outside diameter irrigation pipe connected at the top to a 12 cm outside diameter smooth-walled pipe. Wave data were collected using the same capacitive wave probes as used in the laboratory study, and a third probe was added to better characterize the incident wave characteristics. Wind conditions were monitored throughout the field test. Wave analyses similar to those conducted during the first field study and the model study were used to measure the performance of the prototypes.

The final design can be seen in figures 18 and 19. The composite design performs better on high-steepness waves because it serves to capture some wave sizes between the two sections, resulting in improved dissipation of wave energy.

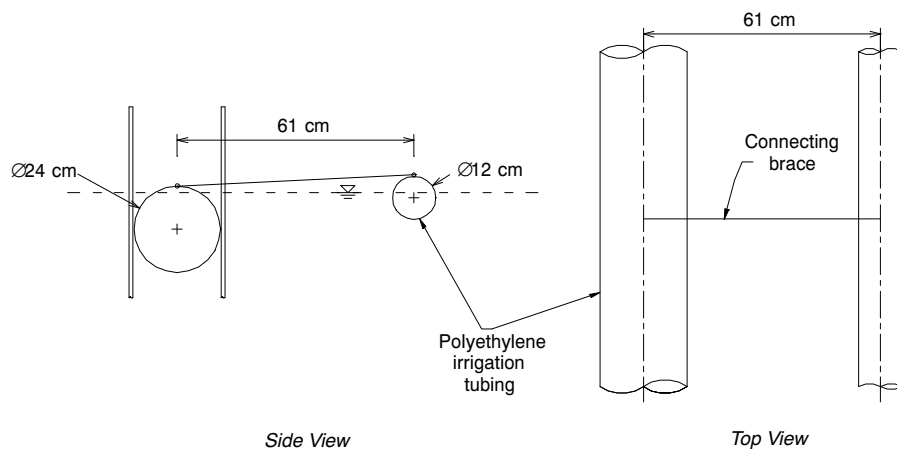


Figure 18. Diagram of final design used in prototype-scale field test.



Figure 19. Temporary prototype-scale field test for composite wave barrier. Waves are coming from the left side of the photo at about a  $20^\circ$  angle to the barrier. Note the visibly lower wave amplitude on the far side of the wave barrier.

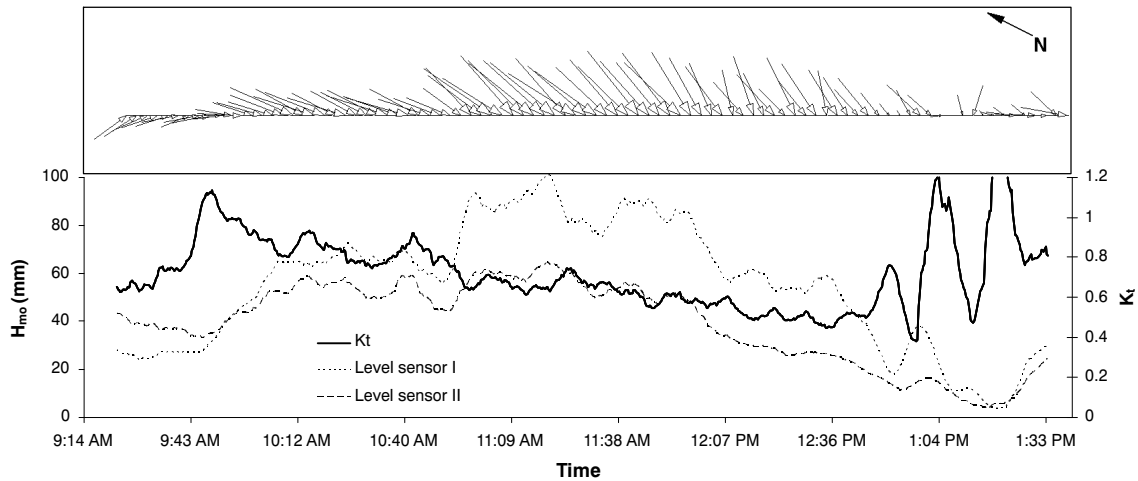


Figure 20. Wind and wave data from short field test in irrigation reservoir. The maximum wind vector length represents a wind of 18 mph.

While it adds some complexity and cost, the composite design has the advantage of eliminating the need for end restraints, since piles driven between the brackets used to maintain the offset of the two pipes will keep the wave absorber in place. The ends of the pipe were covered with plywood, and holes were drilled along the length so that the pipes were filled with water. The added mass of the water and the restricted movement in and out provided by the holes increased the performance of the wave barrier. Using methods similar to those used to analyze wave data from the first field trip and the model study resulted in figure 20, which shows that, for winds that were approximately normal to the barrier (from about 11:00 a.m. to 12:45 p.m.), the reduction in transmitted wave amplitudes ( $1 - \kappa_t$ ) ranged from 40% to 55%. Similar reductions were achieved using a single pipe with  $d = 29$  cm. However, due to the cost and transportation considerations, the composite design was determined to be more desirable.

In figure 20, several things should be noted. The changing wind direction caused the waves to impact the absorber in different directions, resulting in sensor I and sensor II encountering, at times, either incident or reflected waves. The algorithms used to analyze the data took this into account and swapped the treatment of data from the sensors so that  $\kappa_t$  could be correctly calculated. Both early and late in the record, values of  $\kappa_t$  greater than one are seen. These result from low-amplitude waves whose direction was nearly parallel to the wave absorber, causing the level sensors to measure nearly identical wave height. This, combined with measurement error from the sensors, resulted in time periods where the transmission coefficient was greater than one.

Another finding from the field work and the resulting considerations of implementation strategy was that multiple small-diameter pipes bundled together to arrive at larger diameters is preferable from both a logistical and cost standpoint in spite of the additional labor required to bundle the pipes together. A truck can haul 4 914 m rolls of 12 cm pipe. Using a bundle of three pipes with a fourth offset in the previously described configuration means that one truck can deliver enough pipe for 914 m of bank protection. One truck can haul a total of 1219 m of 24 cm pipe, but additional 12 cm pipe would be needed to complete the composite design. Including couplings, the 24 cm pipe costs \$6.40 per meter (in spring 2008). For 29 cm pipe, the cost goes up to \$8.10 per

meter. Using 12 cm pipe, the pipe cost is  $4 \times \$1.31$  per meter = \$5.25 per meter. This cost savings becomes significant when several hundred meters of barrier per pond is considered. It is not possible to accurately factor in transportation cost, since distances from manufacturers to implementation locations can vary widely. However, the ability to protect 914 m of shoreline with one truck delivery will certainly lower transportation costs relative to the other options considered here. In addition, the larger pipe sizes are more commonly available in 6 m sections that must be coupled together. This configuration makes transport of large amounts of pipe more difficult and more costly.

## CONCLUSION

A basic design for a floating wave barrier for use in irrigation reservoirs was determined through scaled model testing in a laboratory wave flume. Various sizes and configurations of cylindrical pipe models were used to determine a final design. Field measurements of wave characteristics allowed the model wave barrier and waves to be scaled so that the results could be applied in a meaningful way. The best combination of performance, cost, and installation logistics was obtained using a pile-restrained floating breakwater with parallel pipes submerged at  $z_d/d = 1.0$  on the upwind side and  $z_d/d = 0.6$  on the downwind side. A subsequent field test validated the conclusion from the laboratory testing that this design can be used to reduce wave energy impacting levees. In the field test, wave amplitudes were reduced by an average of approximately 50%, which translates into 75% reduction in wave energy. It is anticipated that the details of the field implementation will change due to the logistics of installing long sections of barrier, but that the basic design utilizing the offset composite configuration will remain.

Specific conclusions follow:

- As would be expected, for both fixed and floating cases, larger diameter wave barriers had better performance than smaller ones. However, the material and transportation costs of irrigation pipe increase rapidly with diameter, making the use of bundled smaller pipes to arrive at larger diameters a better option than one single large-diameter pipe.

- There is an optimal relative submergence that maximizes the reflection and dissipation characteristics of a given wave barrier design. This value varies based on the type of restraint. For example, fully submerged pile-restrained barriers performed better than fully submerged fixed barriers for a range of wave parameters.
- Of the restraint types tested here, the pile-restrained model was the most effective at attenuating waves.
- The moored arrangement was less effective than pile restraint. The moored design also has the disadvantage of a strong dependence on water level.
- For low-amplitude waves like those considered in the current study, a relative submergence of  $z_d/d = 0.7$  was found to be optimal for the pile-restrained model.
- Bundles of smaller pipes were found to perform in a manner comparable to a single pipe of the same diameter.
- The corrugations on irrigation pipe had no negative effect on wave barrier performance.

#### ACKNOWLEDGEMENTS

We would like to thank Keith Admire at the USDA-NRCS National Water Management Office in Little Rock, Arkansas, for supporting this work. Dennis Carman initiated the work during his tenure with the USDA-NRCS and has continued to be a valuable resource. Glenn Gray provided invaluable technical support for all phases of the work. We also thank M. Altinakar and P. A. Work for valuable input based on their broad experience in coastal and hydraulic engineering.

#### REFERENCES

- Carman, D. 2003. Personal communication, Chief Engineer and Director, White River Irrigation District, Stuttgart, Arkansas, August 12, 2003.
- CERC. 2003. *Shore Protection Manual*. Vicksburg, Miss.: U.S. Army Corps of Engineers, Coastal Engineering Research Center.
- Dean, G. D., and R. A. Dalrymple. 1991. *Water Wave Mechanics for Engineers and Scientists*. Singapore: World Scientific.
- Dean, R. G., and F. Ursell. 1959. *Interaction of a Fixed, Semi-Immersed Circular Cylinder with a Train of Surface Waves*. Tech. Report No. 37. Cambridge, Mass.: Massachusetts Institute of Technology, Hydrodynamics Laboratory.
- Hales, L. Z. 1981. *Floating Breakwaters: State-of-the-Art Literature Review*. Vicksburg, Miss.: U.S. Army Corps of Engineers, Coastal Engineering Research Center.
- Hughes, S. A. 1993. *Physical Models and Laboratory Techniques in Coastal Engineering*. Singapore: World Scientific.
- Isaacson, M. 1993. Wave effects on floating breakwaters. In *Proc. 1993 Canadian Coastal Conference*, 1: 53-65. Ottawa, Ontario, Canada: Coastal Zone Engineering Program National Research Council.
- Longuet-Higgins, M. S. 1980. On the distribution of the heights of sea waves: Some effects of nonlinearity and finite band width. *J. Geophys. Res.* 85(C3): 1519-1523.
- McCartney, B. L. 1985. Floating breakwater design. *J. Waterway, Port, Coastal, and Ocean Eng.* 111(2): 304-318.
- McLaren, R. W. 1981. Preparation of floating breakwater manual. In *Proc. 2nd Conf. on Floating Breakwaters*. B. H. Adey and E. P. Richey, eds. Seattle, Wash.: University of Washington.
- Richey, E. P., and R. E. Nece. 1974. Floating breakwaters: State of the art. In *Proc. Floating Breakwater Conference*, 1-19. Kingston, R.I.: University of Rhode Island.
- USDA-SCS. 1974. A guide for design and layout of vegetative wave protection for earth dam embankments. Tech. Release No. 56. Washington, D.C.: USDA Soil Conservation Service.
- Werner, G. 1988. Experiences with floating breakwaters: A literature review. *PIANC-AIPCN Bulletin* 63(2): 3-30.